

Chapter 3 Structure of the Ru(0001)-(2×2)-3O phase

3.1 Adsorption of oxygen on Ru(0001) – Summary of previous studies

Many studies have been devoted to the adsorption of oxygen on Ru(0001) [39]. With O₂(g) exposures a (2×2)-O phase is formed at an O coverage of 0.25 ML [40], but a (2×1)-O phase at an O coverage of 0.5 ML [41]. The (2×1)-O phase shows the same LEED pattern as that of the (2×2)-O phase because of three different rotational domains [19]. The detailed atomic structures of the (2×2)-O phase [40] and the (2×1)-O phase [41] were determined by dynamical LEED I/E analysis. O atoms always favor the hcp sites. Note that the hcp sites would be occupied by Ru atoms of the next layer in the hcp stacking sequence. Generally, O atoms sit on those sites, where next layer substrate atoms would sit, i.e., hcp sites on hcp(0001) and fcc sites on fcc(111) [42]. The (2×1)-O phase with an O coverage of 0.5 ML was regarded as the saturation phase on Ru(0001) under UHV conditions by exposing O₂ at 300 K [18, 19].

C.H.F. Peden et al. observed that an O phase with an O coverage of 1.0 ML can be formed under high pressure conditions [20–22]. Under UHV conditions, the O phases with O coverages above 0.5 ML can be prepared by using NO₂ [43–46]. The O-rich phases prepared by NO₂ were studied by XPS [43, 45], TDS [43–46], UPS [45], LEED [46] and HREELS [46]. The investigations in Ref. [44, 45] suggested that the saturation coverage of O on the surface is 3.0 ML. However, HREELS and LEED studies on the O-rich phases prepared in the same way as in Ref. [44, 45] determined the saturation coverage of O on the surface to be 1.0 ML [46]. The (1×1) LEED pattern at an O coverage of 1.0 ML was regarded as an indicative of a disordered O overlayer [46]. However, the (1×1) LEED pattern can also be assigned to the formation of a (1×1)-O network.

DFT calculations of the various O phases and LEED I/E analysis for the (1×1)-O phase were conducted [25, 26]. The structures and the adsorption energies of O for the hypothetical (2×2)-3O phase (O coverage = 0.75 ML) and the (1×1)-O

phase (O coverage = 1.0 ML) were determined by DFT calculations. The results of these DFT calculations are summarized in Fig. 3.1. In the (1×1)-O overlayer the hcp site is again the most favorable adsorption site, although the energy difference with respect to the fcc position is only 30 meV. The main result of this theoretical investigation is that the formation of the (1×1)-O phase is still exothermal. Thus, further dissociative adsorption of O₂ on the (2×1)-O phase is hindered for kinetic reasons. The existence of the (1×1)-O phase was confirmed by LEED I/E measurements and calculations [25, 26]. The (1×1)-O phase was prepared by exposing Ru(0001) to NO₂ at 500 K, and the atomic structure of the (1×1)-O surface determined by LEED I/E analysis is in nice agreement with corresponding DFT calculations. The surface saturation coverage of O turned out to be 1.0 ML.

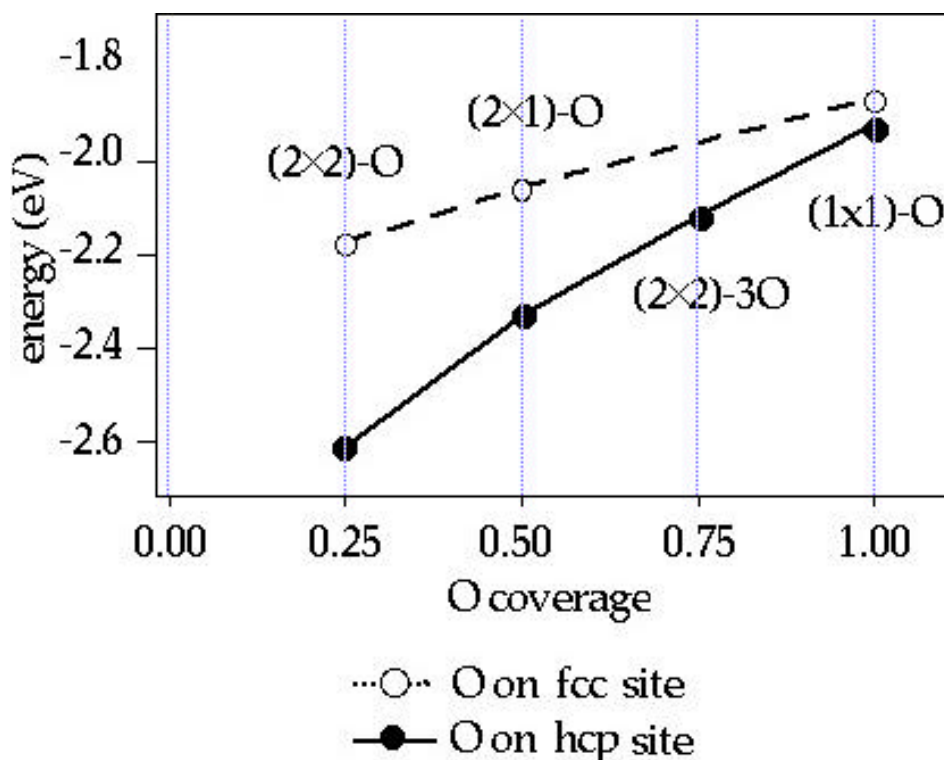


Fig. 3.1. Adsorption energy of O as a function of O coverage. The zero point of the energy axis corresponds to the half binding energy of an O₂(g) molecule [40].

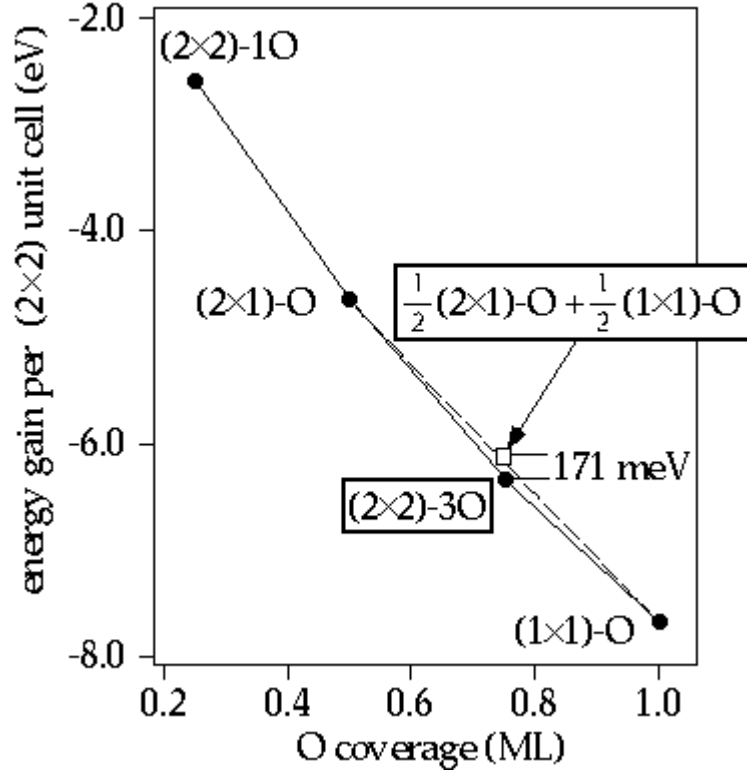


Fig. 3.2. Total energy of the (2x2)-3O phase and a mixed phase of the (2x1)-O and the (1x1)-O overlayer per (2x2) unit cell.

According to DFT calculations, the formation of the (2x2)-3O overlayer is also exothermal [25]. Here, O adsorption in the hcp site was predicted. It can be excluded that at this O coverage a mixed phase of the (2x1)-O and the (1x1)-O networks is formed, instead of a well-defined (2x2)-3O overlayer. In Fig. 3.2, the theoretically determined adsorption energy of the (2x2)-3O phase per (2x2) unit cell is compared with that of the mixed phase of the (2x1)-O and the (1x1)-O overlayers. The (2x2)-3O phase is by 171 meV per (2x2) unit cell more stable than the [(2x1)-O + (1x1)-O] mixed phase.

STM and HREELS studies verified that the (2x2)-3O phase is indeed formed at an O coverage of 0.75 ML [47]. They proposed that the (2x2)-3O phase is a (2x2) vacancy structure (an unoccupied hcp site of the (1x1)-O overlayer is described as a vacancy).

3.2 Motivation of studies on the Ru(0001)-(2×2)-3O phase

CO oxidation on metal surfaces is one of the most widely studied subjects in surface chemistry as a model system of heterogeneously catalyzed reactions.

Two reaction mechanisms have been proposed for the catalytic CO oxidation, the so-called ‘Langmuir-Hinshelwood mechanism’ [48, 49], and the ‘Eley-Rideal mechanism’ [50]. Both mechanisms can be identified using the molecular beam technique [51]. According to the Langmuir-Hinshelwood mechanism, O₂ adsorbs dissociatively on the surface, while CO adsorbs molecularly. Since the mobility of CO is much higher than that of adsorbed O atoms, CO diffuses on the surface, until it encounters a thermally activated O. An activated CO₂-like complex may form before recombination and desorption as CO₂(g). The catalytic CO oxidation on the Pt group metal surfaces is explained within the Langmuir-Hinshelwood mechanism [52–55]. Most of the heterogeneous catalytic reactions are considered to occur via this mechanism [51].

The Eley-Rideal mechanism assumes that CO molecules approaching the surface from the gas phase react directly with the chemisorbed O atoms on the surface. The residence time of a CO molecule on the surface can be assumed to be zero. There is, however, no experimental evidence of real catalytic reactions that can take place via Eley-Rideal mechanism [51]. Only the recombination of D in the gas phase with H on Ru(0001) [56], the protonation of N(C₂H₄)₃N on Pt(111) [57], the reaction of Cl in the gas phase with H on Ag(111) [58] can occur with the Eley-Rideal mechanism.

The mechanism of the CO oxidation on the (1×1)-O phase over Ru(0001) is not clearly understood. During 1986–1991, studies about the interaction of Ru(0001) with oxygen and CO under high pressure conditions were published [20–22]. Under steady-state conditions, the CO(ad) and CO₂(g) were monitored with IRAS. Under ‘reducing condition’, i.e., if the pressure of CO is 16 torr, and the pressure of O₂ is just 0.5 torr, CO adsorbs on the surface. In this case, the CO to CO₂ conversion probability is quite low. CO oxidation under ‘reducing condition’ can be explained

via the Langmuir-Hinshelwood mechanism, because CO adsorption can be detected. The low reactivity under this condition was rationalized in terms of the higher binding energy of O on Ru. Under ‘oxidizing condition’, i.e., if the O₂ pressure is increased to 8 torr, no CO adsorption on the surface is observed, although the CO to CO₂ conversion probability turned out to be about 30 times higher than that under the ‘reducing condition’. After the reaction under the ‘reducing condition’, the O coverage turned out to be below 0.5 ML, while the O coverage was 1 ML after treatment under the ‘oxidizing condition’. The results from the experiments under ‘oxidizing condition’ left out a question concerning the actual CO oxidation mechanism. Since no CO adsorption was detected during the reaction, CO oxidation reaction was suggested to proceed via the Eley-Rideal mechanism. These surprising results triggered further experimental and theoretical investigations.

DFT calculations revealed that the Eley-Rideal mechanism cannot account for such a high activity for the CO oxidation at the high pressure range [59, 60]. The theoretically calculated CO to CO₂ conversion probability on the (1×1)-O phase via the Eley-Rideal mechanism is about 3×10^{-6} times smaller than the experimentally determined value [60].

To explain the experimentally found high activity for the CO oxidation without any detectable CO(ad) under the ‘oxidizing condition’, the theoretical study suggested the CO adsorption in vacancies of the (1×1)-O phase and subsequent reaction via the Langmuir-Hinshelwood mechanism [59, 60]. Theoretically, CO can adsorb in the vacancies with the binding energy of about 0.85 eV [59].

To prove this mechanism experimentally, the adsorption geometry of CO molecules on vacancies of the (1×1)-O overlayer should be studied. The (2×2)-3O phase can be envisioned as a (2×2) vacancy structure of the (1×1)-O phase. The structure and reactivity of CO oxidation on vacancies of the (1×1)-O overlayer can be studied indirectly by investigating the (2×2)-3O phase.

3.3 Preparation of the Ru(0001)-(2×2)-3O phase

The Ru(0001) sample was cleaned by cycles of sputtering at 700 K and oxidation at 1100 K. AES could not quantify the cleanness of the surface, because the main contaminant, C, has its main peak at the same position (273 eV) as Ru [61]. 30 L of O₂ was dosed at room temperature, and a thermal desorption experiment was conducted. The sample was considered to be clean, when the C+O recombination peak between 700 K and 1100 K became negligibly small. The LEED pattern of a clean sample exhibited sharp spots with high intensities and low background intensities.

O₂ or NO₂ can be utilized for the preparation of high coverage O phases. High doses of O₂, about 10⁶ L of O₂, should be used at a sample temperature of 500 K to prepare the (1×1)-O phase on Ru(0001) [23]. The drawback of this procedure is that a quite long time is needed for a UHV chamber to recover a base pressure of 10⁻¹⁰ mbar.

The other preparation route to produce high coverage O phases is to use NO₂ as a source of atomic O. NO₂ is a radical, and it is more easily dissociated to NO and O on metal surfaces than O₂ due to its lower dissociation enthalpy. The bond strength of ON–O is 305 kJ/mol, while 498 kJ/mol for O–O [62]. N₂O can not produce high coverage O phases, although its dissociation enthalpy (for N₂–O, 167 kJ/mol at room temperature [62]) is lower than that of NO₂, because it does hardly adsorb on the surface. In contrast to O₂, just small amounts of NO₂ are needed for the preparation of the O phases with coverages above 0.5 ML. For example, only 40 L of NO₂ is required for preparing the (1×1)-O at the sample temperature of 500 K [23].

NO₂ molecular radical has been used to produce higher O coverages, which are hardly prepared with O₂ under UHV conditions. For instance, on Pt(111) [63, 64] and Pd(111) [65], 0.75 ML or 1.4 ML of O can be accumulated by using NO₂, respectively. Note that the (2×2)-O phase (O coverage = 0.25 ML) is the quasi-

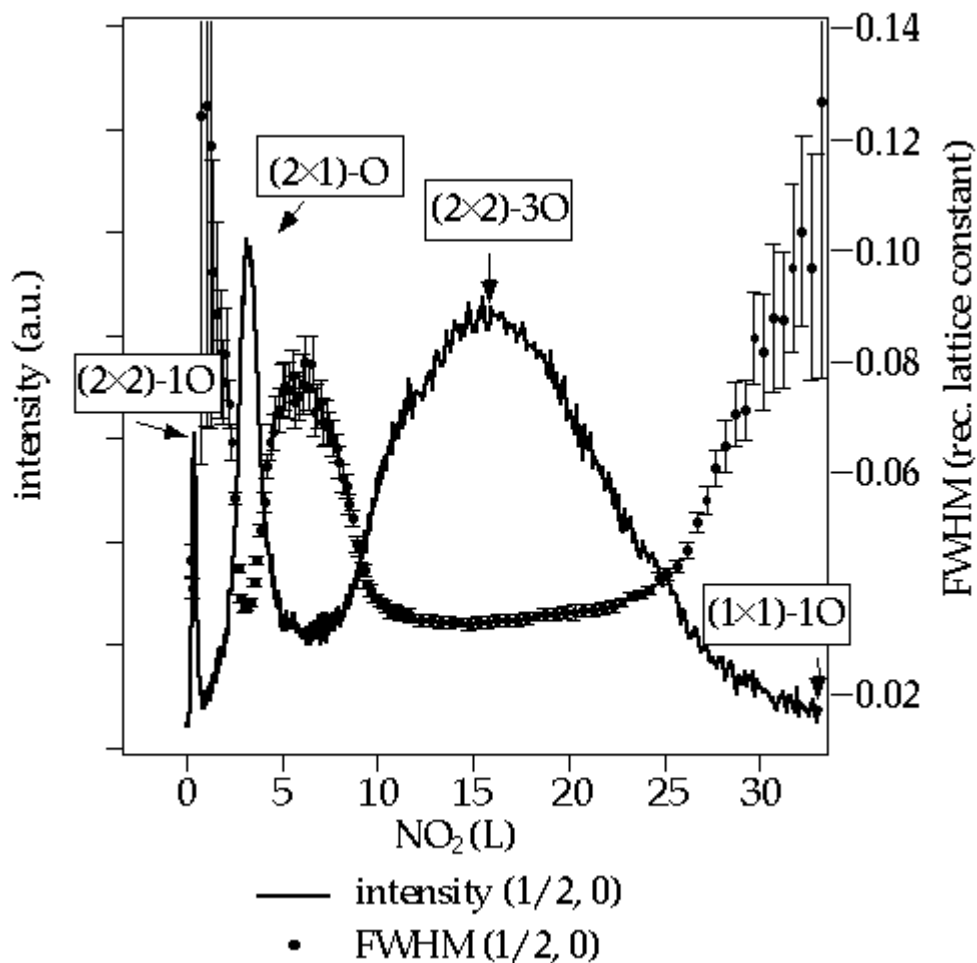


Fig. 3.3. Variation of a (2×2) fractional-order beam intensity and FWHM (Full width of half maximum) upon exposure to NO₂ measured by S. Schwegmann. The energy of the primary electrons was 42 eV. The sample temperature was 500 K.

saturation phase, when O₂ is used for the preparation under UHV conditions on both surfaces [66–68]. However, using NO₂ has also disadvantages. NO₂ is toxic and not easily pumped out. I.J. Malik et al. warned that NO₂ corrodes Cu gaskets [44].

In the present work, we used NO₂ for the preparation of the (2×2)-3O structure. One additional advantage of using NO₂ is that one can follow the change of the LEED pattern during the formation of the (2×2)-O, the (2×1)-O, the (2×2)-3O and the (1×1)-O phase. Using the shower system, in-situ LEED measurements during the preparation are impossible.

NO_2 was exposed to the clean Ru(0001) surface at 500 K. During dosing of NO_2 , the intensity of a (2×2) fractional-order beam was recorded. A temperature of 500 K was chosen, because the sample temperature for this measurement should be sufficiently high to remove NO, but on the other hand, low enough to allow for a significant residence time of NO_2 on the surface. Also, the sample temperature has to be lower than the order-disorder phase transition temperatures of the O phases in order to observe the additional spots caused by the O. Fortunately, the phase transition temperatures for the (2×2) -O and the (2×1) -O phase are 870 K and 580 K, respectively [69]. From the Fig. 3.3, three differently ordered phases with the (2×2) LEED pattern can be identified by three distinct peaks in the intensity profile. In the transition regions, broadening of the spot profile (or increase of FWHM) is observed, indicating the formation of many phase-antiphase boundaries. After the formation of the third (2×2) ordered phase, further dosing of NO_2 leads to the formation of the (1×1) -O phase, which is suggested by the disappearance of the (2×2) superstructure. At least three different O phases with a (2×2) or a (2×1) periodicity exist on Ru(0001). We can assign the first two peaks of Fig. 3.4 to the (2×2) -O and the (2×1) -O. The third peak corresponds to the (2×2) -3O phase with an O coverage of 0.75 ML.

3.4 Structure determination of the Ru(0001)- (2×2) -3O surface by LEED I/E analysis

The detailed surface geometry of the (2×2) -3O phase was studied by using quantitative LEED I/E analysis. The LEED I/E curves from three integer-order beams and five fractional-order beams were collected with the total energy range of 1394 eV. The (2×2) vacancy structure was tested as a model structure of the (2×2) -3O phase. The (2×2) vacancy structure is the only model for the (2×2) -3O phase, assuming that O atoms exclusively occupy hcp sites.

In Fig. 3.4, the best-fit structure of the (2×2)-3O phase is shown. The overall R_p is 0.25, which indicates a nice agreement between theory and experiment. The experimental and the calculated LEED I/E curves are compared in Fig. 3.5.

The bond lengths of Ru–O are 1.98 Å and 2.03 Å. The two Ru–O bond lengths are due to the lateral shift of O atoms. The average value of Ru–O bond length is 2.00 Å. In Fig. 3.7, the structural parameters of the (2×2)-O, the (2×1)-O, the (2×2)-3O and the (1×1)-O phase are compared [70]. One would expect an expansion of the Ru–O bond length with increasing O coverage, because the binding energy of O decreases with increasing O coverage. The experimentally determined Ru–O bond length is, however, almost independent of O coverage. The average value of the first interlayer distance (d_{12}) of Ru for the (2×2)-3O phase is 2.21 Å, which is slightly expanded with respect to the bulk value. There is a considerable contraction of d_{12} for the clean surface. Such a contraction of d_{12} can very often be observed on clean metal surfaces, since the topmost surface atoms are lower-coordinated than bulk atoms. The O adsorption induces a d_{12} expansion, because O as an electronegative species is able to withdraw electrons from the bonding band of the substrate. This weakens the attraction between the first layer and the second layer of the substrate [71]. Hence, d_{12} increases with increasing O coverage on the surface. Our experimentally determined d_{12} value of the (2×2)-3O nicely fits this trend. The expansion of d_{12} for the (2×2)-3O phase was also found in the DFT calculations [72].

A buckling of 0.08 Å occurs in the second Ru layer. The second-layer Ru atoms move towards the three attached first-layer Ru atoms, which are only coordinated to two O atoms. Within this four-Ru cluster, the layer distance (2.15 Å) is almost bulk-like (2.14 Å). The first-layer Ru atoms, which are attached to three O atoms, move slightly inwards by 0.02 Å. The averaged layer distance (2.21 Å) between this first-layer Ru atom and the three attached Ru atoms in the second layer directly below is, however, still substantially expanded with respect to the bulk value.

The O atoms move by 0.05 Å radially away from the high-symmetry hcp sites

towards the bridge sites, in order to optimize the electronic environment for the O atoms. Note that in the unrelaxed (2×2) -3O overlayer, one Ru atom is coordinated to three O atoms, whereas the other three Ru atoms in the unit cell are only attached to two O atoms. From a recent LEED analysis of the O phases on Ru($10\bar{1}0$), it was concluded that O does not like to share Ru atoms with other O atoms [73]. Therefore, it seems plausible to attribute the observed lateral relaxation of O atoms to this effect.

The structure of the (2×2) -3O phase was also determined by Gsell et al., who used

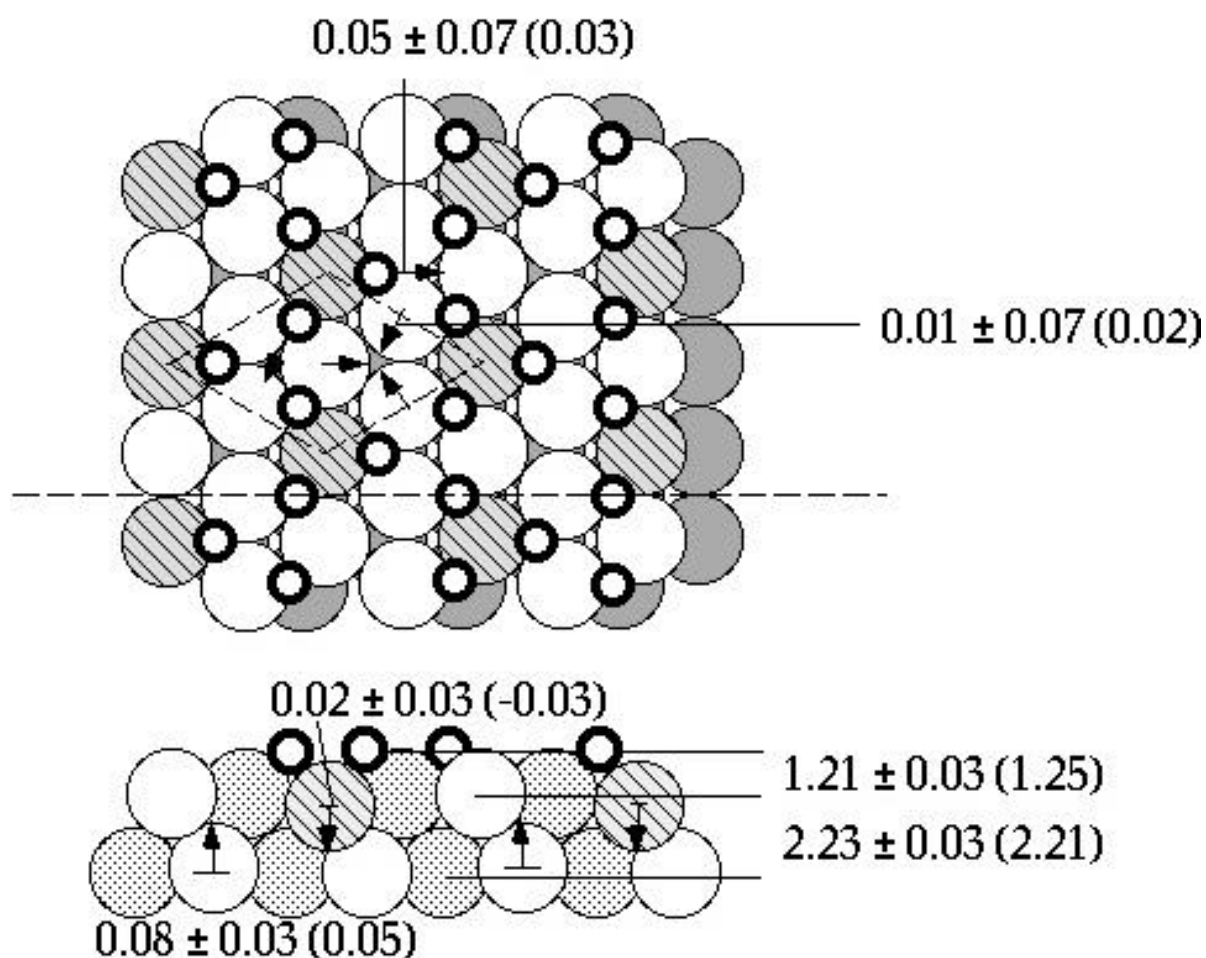


Fig. 3.4. Best-fit geometry of the Ru(0001)- (2×2) -3O phase determined by LEED I/E analysis. The values are given in Å. The structural parameters determined by Gsell et al. [74] are given in parentheses.

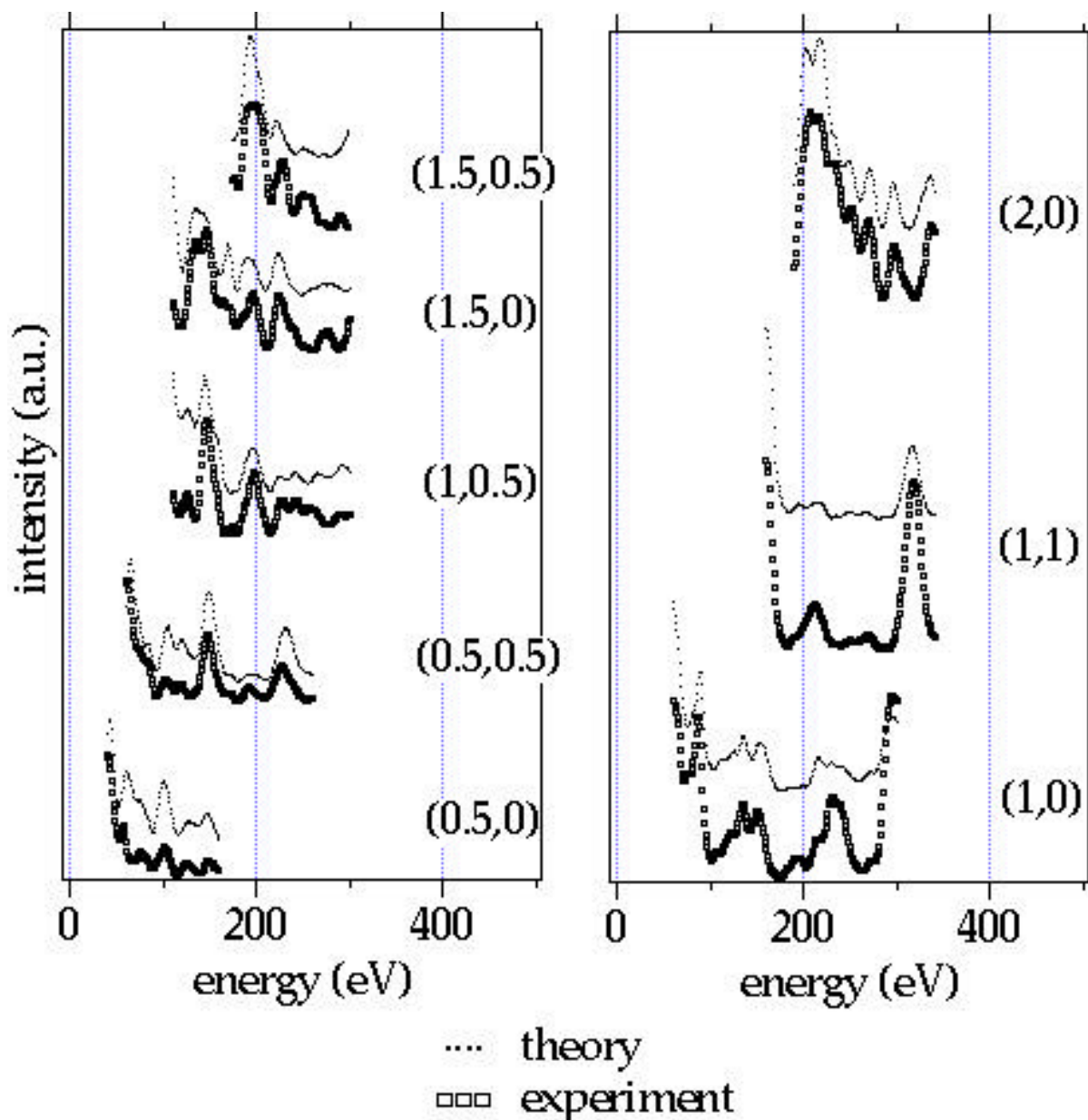


Fig. 3.5. The experimental LEED I/E curves are compared with calculated ones for the best-fit structure of the Ru(0001)-(2×2)-3O surface ($R_p = 0.25$).

quantitative LEED I/E analysis [74]. There, a d_{12} expansion with respect to the bulk value was also found. The Ru–O bond length turned out to be independent of O coverage, in agreement with our results. The authors of Ref. [74] also found lateral displacements of O and first-layer Ru, and the buckling of the second layer to the

×

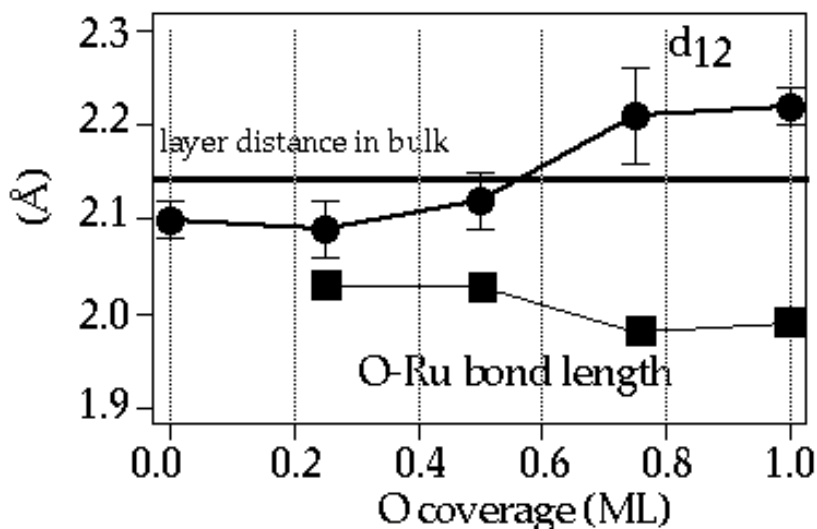


Fig. 3.6. The average values of d_{12} and Ru–O distance for the various O phases on Ru(0001) [70].

same directions as our work. The first-layer buckling from Ref. [74] is, however, in opposite direction to our result.

3.5 CO adsorption on the Ru(0001)-(2×2)-3O surface

3.5.1 CO adsorption on O-precovered Ru(0001)

Adsorption properties of CO on metal surfaces have been widely investigated [39]. The CO adsorption mechanism can be explained with the Blyholder model (Fig. 3.8) [75]. In the Blyholder model, the 5σ orbital (HOMO; the highest occupied molecular orbital) and the $2p$ orbital (LUMO; the lowest unoccupied molecular orbital) of CO play the dominating role for the chemisorption. Electrons are donated from the 5σ orbital to the d orbital of the substrate with s symmetry and electrons from d orbitals with p symmetry are backdonated to the $2p$ orbital of CO. It is generally believed that the p backdonation governs the bond strength of CO to the metal surfaces.

CO molecules occupy on-top, bridge or threefold-hollow sites on fcc(111) or

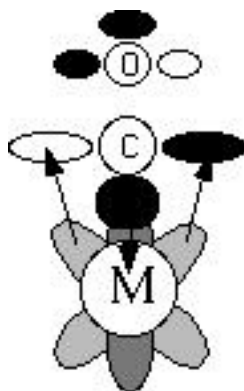


Fig. 3.7. Blyholder model of CO adsorption in the on-top position.

hcp(0001) surfaces [39]. There is no simple rule to predict adsorption sites of CO on metal surfaces. Detailed theoretical investigations and experimental evidences are necessary to verify the adsorption site of CO.

CO adsorption on Ru(0001) takes place with an initial sticking coefficient of about 0.8 at room temperature [76]. The atomic adsorption site of CO was determined by LEED I/E analysis [77, 78]. At a CO coverage of 0.33 ML, a $(\sqrt{3}\times\sqrt{3})R30^\circ$ -CO structure is formed, in which CO molecules sit in on-top positions. The saturation coverage of CO is about 0.7 ML [79]. A DLEED study showed that the on-top configuration is also favored at the CO coverage below 0.25 ML [80].

Several CO+O coadsorption phases are found on Ru(0001), whose detailed structures were investigated by LEED and IRAS (Fig. 3.10). On the (2×2) -O phase, CO coadsorption led to the (2×2) -(O+CO) [81] and the (2×2) -(O+2CO) phases [82]. In the both coadsorption systems, O atoms do not change their adsorption sites from the hcp sites. In the (2×2) -(O+CO) phase, CO molecules sit in on-top positions, i.e., the same positions as in the pure CO phases. In the (2×2) -(O+2CO) phase, additional CO molecules sit on fcc sites without changing the adsorption sites of the precovered (2×2) -(O+CO) surface [82]. The (2×1) -O overlayer also allows for the additional adsorption of CO.

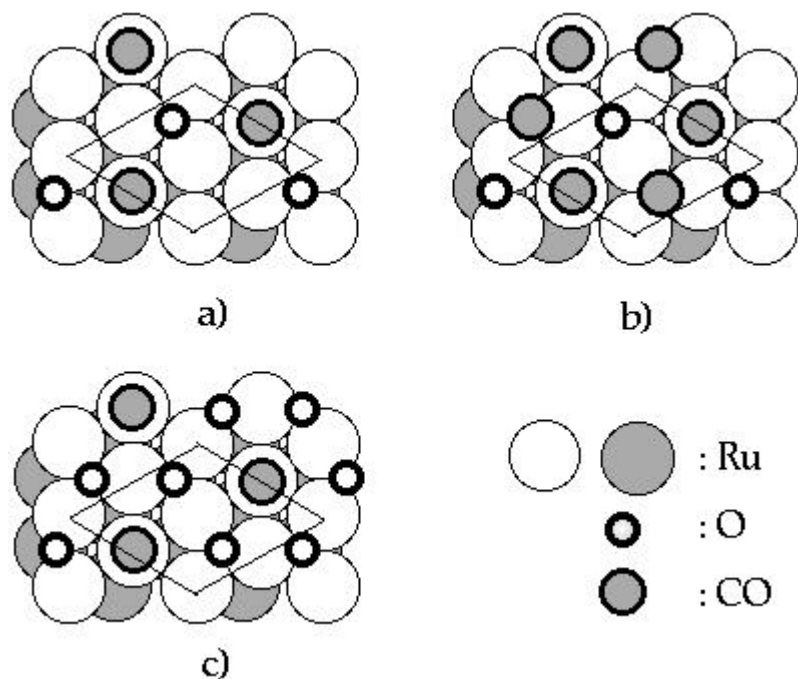


Fig. 3.8. Various experimentally found O+CO coadsorption phases on Ru(0001). a) (2×2) -(O+CO) [81], b) (2×2) -(O+2CO) [82], c) (2×2) -(2O+CO) [83].

At a sample temperature above room temperature, the (2×2) -(2O+CO) is formed [83]. The O atoms form a network with fcc and hcp sites, and CO occupies the on-top position. This change of the O adsorption site opens on-top sites, on which CO can adsorb; this is not possible with the (2×1) -O without the rearrangement of the O atoms. The energy penalty from the site change of the O atoms is compensated by allowing CO adsorption on the on-top site.

CO adsorption on the (1×1) -O overlayer cannot be detected at sample temperatures above 50 K [17].

3.5.2 Results for CO adsorption on the Ru(0001)- (2×2) -3O phase

After the preparation of the (2×2) -3O phase, CO was dosed at sample temperatures

between 100 K and 300 K. This does not cause any variation of the LEED pattern.

In order to investigate the CO adsorption on the (2×2)-3O overlayer in more detail, LEED I/E curves were measured before and after dosing 10000 L of CO at various sample temperatures. The LEED I/E curves do not change after dosing CO. This precludes CO adsorption in well-defined sites. However, CO may form a disordered phase. A disordered CO layer should decrease the absolute intensities of LEED spots, which was not observed. Therefore, we conclude that CO does not adsorb at all on the (2×2)-3O surface.

From the ab-initio calculations it was predicted that CO adsorption in vacancies of the (1×1)-O overlayer is exothermal with an adsorption energy of 0.85 eV [59, 84]. To make this compatible with our LEED result, a kinetic barrier for the CO adsorption on the (2×2)-3O phase has to be invoked. A theoretical investigation has confirmed an activation barrier for the CO adsorption. The activation energy for the CO adsorption in the (2×2)-3O phase was determined to be about 0.3 eV [84].

We studied this phase, because it was expected that the mechanism of the CO oxidation on the (1×1)-O phase can be identified by investigating the (2×2)-3O phase. However, we found out that no CO adsorption takes place on the (2×2)-3O overlayer, which can be rationalized by the high activation energy for the CO adsorption [84].

The attempt frequency of CO to overcome this activation barrier increases with increasing CO pressure. In the high pressure range, therefore, large amounts of CO molecules may adsorb on vacancies of the (1×1)-O phase, which can then recombine with neighboring O atoms to CO₂. Although we could not observe the adsorption of CO on the (2×2)-3O surface under UHV conditions, the vacancy of the (1×1)-O overlayer may play an important role for the CO oxidation in the high pressure regime.